Molecular Crystals and Liquid Crystals Science and Technology. Section A. Molecular Crystals and Liquid Crystals

Publication details, including instructions for authors and subscription information:
http://www.tandfonline.com/loi/gmcl19

Laser Raman Study of Terepthalylidene-bis-p-n-Decylaniline (TBDA)

S. K. Dash [a] , Ranjan K. Singh [b] , P. R. Alapati [a] & A. L. Verma [b]

[a] Department of Physics, North Eastern Regional Institute of Science and Technology, Itanagar, 791109, India

[b] Department of Physics, North Eastern Hill University, Shillong, 793 022, India

Version of record first published: 04 Oct 2006

To cite this article: S. K. Dash, Ranjan K. Singh, P. R. Alapati & A. L. Verma (1998): Laser Raman Study of Terepthalylidene-bis-p-n-Decylaniline (TBDA), Molecular Crystals and Liquid Crystals Science and Technology. Section A. Molecular Crystals and Liquid Crystals, 319:1, 147-158

To link to this article: http://dx.doi.org/10.1080/10587259808045655

Mol. Cryst. Liq. Cryst., Vol. 319, pp. 147–158
Reprints available directly from the publisher
Photocopying permitted by license only

Laser Raman Study of Terepthalylidene-bis-*p*-*n*-Decylaniline (TBDA)

S. K. DASH[a], RANJAN K. SINGH[b], P. R. ALAPATI[a] and A. L. VERMA[b,*]

[a] *Department of Physics, North Eastern Regional Institute of Science and Technology, Itanagar-791 109, India;*
[b] *Department of Physics, North Eastern Hill University, Shillong-793 022, India*

(Received 1 February 1997; In final form 15 July 1997)

The Raman spectra of Terepthalylidene-bis-*p*-*n*-declyaniline (TBDA), have been recorded as a function of temperature in the temperature range from 55.0°C (solid) to 199.0°C (isotropic liquid) in the 1100–1200 cm^{-1} and 1520–1650 cm^{-1} regions. The precise values of peak positions, integrated intensities and linewidths of some selected Raman bands have been obtained by deconvoluting the bands. The changes in the molecular alignment and its effect on inter/intra molecular interactions at two particular phase transitions *viz.*, solid–smectic *G* (K–S_G) and smectic *I*–Smectic *C* (S_I–S_C) have been discussed on the basis of variation in the Raman spectral parameters with temperature. From detailed considerations, it is inferred that the increased orientational/vibrational freedom of long alkyl chain on the core is responsible for major spectral changes at the K–S_G transition while the changes in the intramolecular interactions of the core part with increased fluidity, is responsible for spectral anomalies at the S_I–S_C transition.

Keywords: Liquid crystals; Laser Raman spectroscopy; molecular dynamics; S_I–S_C transition

1. INTRODUCTION

Raman spectroscopy has proved to be an important technique to investigate the phase transitions in view of the fact that variation of certain physical quantities affect the polarizability tensor and results in changes in the measurable parameters of certain vibrational modes of the system. The measurement and analysis of linewidths and peak positions yield information about the structure and dynamics of the system undergoing phase

*Corresponding author. Fax: +91-364-250076; e-mail: verma@nehus.ren.nic.in

transition. However, the analysis of the integrated intensity is no less important and may provide the crucial information about the fluctuation of appropriate physical quantities undergoing changes during transition.

Raman spectroscopic technique has extensively been applied to study the phase transitions in liquid crystals [1 – 3]. In almost all these studies, major attention has been focused to analyze either the lattice mode region [1 – 6] or the conformationally sensitive alkyl chain mode region (200 – 900 cm^{-1}) [6 – 10]. Lattice mode region shows abrupt changes in intensity of certain modes with increasing temperature [1 – 6] which is associated with decrease in intermolecular interactions as well as positional ordering. Abrupt changes in intensity also occur in the alkyl chain mode region [6 – 10] and it has been ascribed to the fact that at higher temperatures the increased freedom between different molecular layers allows orientational and translational motions of the long alkyl tail along their molecular long axis. Although Raman spectra of TBBA [12 – 13] have been reported in different smectic and nematic phases in the 1550 – 1650 cm^{-1} region (associated with the core part of the TBBA molecule), but any detailed discussion of the spectral changes associated with the core part of the molecule is lacking.

It is therefore worthwhile to correlate the changes in the spectral features associated with the core part of the molecule as a function of temperature with inter/intra molecular interactions and the resulting dynamics of the core. In the present study we have also attempted to discuss systematically the effect of increased amplitude of vibrations of the long alkyl chain on the core and the structural phase transitions.

2. EXPERIMENTAL DETAILS

TBDA was synthesized by the standard procedure [14 – 15] and recrystallized from an absolute ethanol-benzene mixture repeatedly until the observed transition temperatures were found constant. Special precautions were taken to prevent atmospheric hydrolysis as the compounds of this homologous series are prone to decomposition due to prolonged heating at high temperatures. The transition temperatures were obtained using DSC and Polarizing microscope equipped with a hot stage and found to be in excellent agreement with literature values [15].

The samples for Raman studies were contained in a 0.5 mm diameter capillary tube, sealed and placed in an evacuated chamber inside a high temperature cell. The temperature was continuously monitored and measured accurately within $\pm 0.2°C$ with a Copper-Constanton thermo-

couple placed in close contact with the sample. The Raman spectra were recorded at different temperatures, starting from 55.0°C (solid phase) to 199°C (isotropic phase) in the $1100-1220\,cm^{-1}$ and $1520-1675\,cm^{-1}$ regions on a Spex Ramalog 1403 double monochromator equipped with RCA-31034 photomultiplier tube and CCD detector using 488.0 nm line of Ar^{+}-laser as an excitation source. In order to avoid laser heating of the sample, very low laser power (20–30 mW) was employed. Slit combination of 200–400–400–200 μ, scanning increment of $0.3\,cm^{-1}$ and integration time of 0.5 sec were found suitable to record the spectra with reasonably good signal to noise ratio. The mentioned Raman modes are comparatively isolated and sharp and the uncertainty in their peak positions is within $\pm 0.1 cm^{-1}$. We had made 3–4 measurements near phase transition with very high reproducibility of data (uncertainty in peak positions within $\pm 0.20\,cm^{-1}$ while band areas and linewidth (FWHM) are accurate to ± 2%).

3. RESULTS AND DISCUSSIONS

The molecular structure and transition temperatures of TBDA are given below:

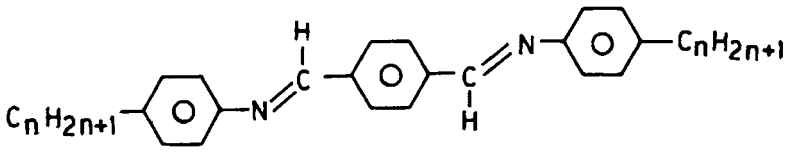

$$\text{Solid} \xleftrightarrow{73^{\circ}C} S_G \xleftrightarrow{120^{\circ}C} S_F \xleftrightarrow{148.4^{\circ}C} S_I \xleftrightarrow{153.4^{\circ}C} S_C \xleftrightarrow{188.3^{\circ}C} S_A \xleftrightarrow{190.2^{\circ}C} I_{so}$$

TBDA molecule can be considered as made up of two distinct parts; one, core consisting of three benzene rings strongly bonded by Schiff base linkages (—C(H)=N—) and the other, saturated long alkyl chains of zig zag structure [16–17] attached to both ends of the core. The Raman spectra of TBDA recorded in the $1100-1220\,cm^{-1}$ and $1520-1675\,cm^{-1}$ regions at seven different temperatures covering all the liquid crystal phases are shown in Figure 1. A tentative assignment of all the peaks in the above regions has been made on the basis of their depolarization ratios, expected group frequencies and reported assignment of similar Schiff base compounds [18] and is given in Table I. It is seen from Figure 1 that the bands are slightly overlapped in the wings. In order to obtain precise values of integrated

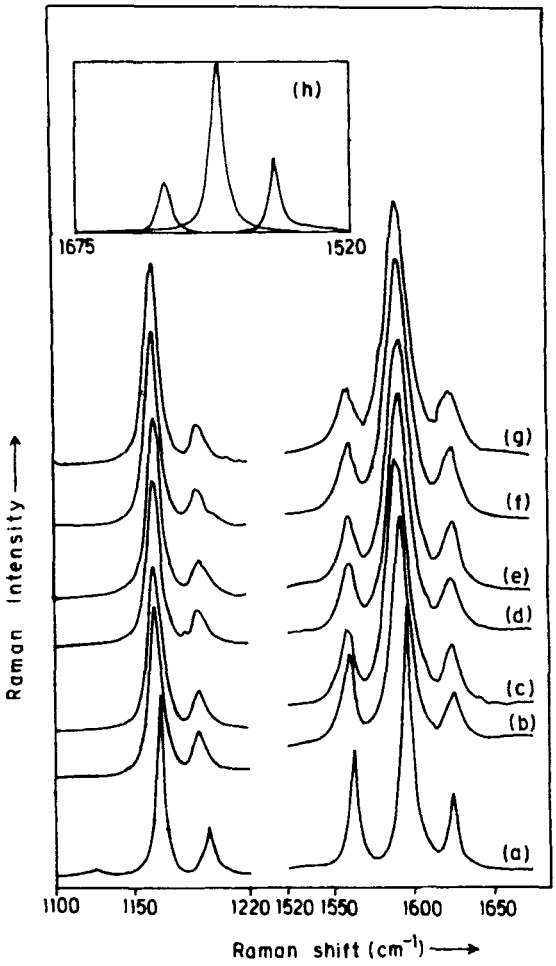

FIGURE 1 Raman spectra in the 1100–1220, and 1520–1675 cm^{-1} regions at different temperatures; (a) 62°C, (b) 90°C, (c) 145°C, (d) 150°C, (e) 163°C, (f) 190°C, (g) 199°C, and (h) one representative deconvoluted spectrum in the 1520–1675 cm^{-1} region at 62°C given as an inset.

intensity, linewidth and peak position, the peaks have been deconvoluted by fitting the spectra in the 1100–1220 cm^{-1} and 1520–1675 cm^{-1} regions to two and three Lorentzian profiles, respectively, at every temperature. The representative deconvoluted spectra for the 1520–1675 cm^{-1} region at 62.0°C are also given along with other recorded spectra in Figure 1. The percent contribution of the individual bands to their respective overlap spectral region has been calculated and taken as a measure of integrated

TABLE I Assignment and depolarization ratios of Raman bands of TBDA in the 1100–1200 cm^{-1} and 1520–1650 cm^{-1} spectral regions

Band position	*Assignment*	*Dep. ratio*
1165 cm^{-1} (s)	Aromatic C—H in-plane bending mode (ν_{9a})	0.28
1195 cm^{-1} (sm)	Aromatic C—N stretching mode ($\nu_{\phi-N}$)	0.35
1417 cm^{-1} (m)	Semicircle stretching of C—C aromatic benzene ring (ν_{19b})	0.43
1503 cm^{-1} (m)	Semicircle stretching of C—C aromatic benzene ring (ν_{19a})	0.48
1563 cm^{-1} (sm)	Quadrant stretching of benzene ring ($\nu_{8a'}$)	0.34
1594 cm^{-1} (vs)	Quadrant stretching of benzene ring (ν_{8a})	0.30
1625 cm^{-1} (sm)	C=N stretching mode $\nu_{C=N}$	0.33

vs – very strong, s – strong, sm – strong medium, m – medium.

intensity. The values of integrated intensities, linewidths, and peak positions obtained for all the bands at different temperatures are given in Table II. It is to be mentioned here that integrated intensity measurement with respect to an internal standard is avoided because doping may change the characteristics of the sample. Again, as stated earlier, in the present study we are interested in analyzing the structural disorder of the core at different transition temperatures which is normally considered as a rigid part of the molecule. Therefore five prominent Raman bands (1165 cm^{-1}, 1195 cm^{-1}, 1563 cm^{-1}, 1594 cm^{-1} and 1625 cm^{-1}) associated with the core of the TBDA molecule have been chosen on the basis of their assignment (see Tab. I), so that the relevance of any spectral changes to the behaviour of the core can easily be seen.

A. Effect of Long Alkyl Chain on the Core at the Solid-smectic *G* Transition

The variation of integrated intensity, linewidth and peak position of the 1165, 1195, 1563, 1594 and 1625 cm^{-1} bands with temperature is presented in Figures 2, 3 and 4 respectively. These figures reveal that the first anomaly in the integrated intensity, linewidth and peak position profiles occurs for all the Raman bands at 73°C, which has already been reported [15] as the $K-S_G$ transition temperature in TBDA. The $K-S_G$ phase transition is an example of a transition between two well defined three dimensional structures, the only difference being that S_G is a highly viscous liquid crystal phase. Although the alkyl chain part of the molecule attains higher degree of orientational freedom and more vibrational freedom at melting involving a phase transition from crystalline to crystal like smectic phase

TABLE II The percent contribution of the integrated intensities of the 1165, 1195, 1563, 1594 and 1624 cm^{-1} bands to the total integrated intensity of their respective spectral regions (1100 – 1200 cm^{-1}, and 1520 – 1675 cm^{-1}) along with their peak positions at different temperatures

Temperature in °C	*liquid crystals phases*	*Raman modes* 1165 cm^{-1}			1195 cm^{-1}			1563 cm^{-1}			1594 cm^{-1}			1625 cm^{-1}		
		II	*PP*	*LW*	*II*	*PP*	*LW*	*II*	*PP*	*LW*	*II*	*PP*	*LW*	*II*	*PP*	*LW*
55.0		79.5	1165.4	5.90	20.5	1195.6	7.43	24.9	1562.8	6.35	59.1	1594.6	7.84	16.0	1624.6	7.56
62.0	Solid	79.4	1165.5	6.00	20.4	1195.7	7.58	24.4	1562.6	6.40	59.2	1594.8	8.64	16.4	1624.9	7.80
69.0		79.6	1165.7	6.20	20.6	1195.7	8.00	24.0	1561.9	6.62	59.5	1594.3	8.82	16.5	1624.5	7.90
73.0		80.0	1162.5	10.0	20.6	1190.5	9.40	23.9	1159.7	7.70	63.0	1592.3	12.2	13.1	1624.6	10.0
75.0	S_G	80.1	1162.3	9.90	19.9	1190.4	9.30	23.4	1559.5	7.84	63.4	1592.5	12.3	13.2	1624.8	10.5
90.0		80.8	1162.3	10.2	19.2	1190.6	9.64	23.0	1559.9	8.04	63.2	1592.2	13.7	13.8	1624.8	11.6
115.0		81.0	1162.6	10.0	19.0	1190.4	9.61	22.8	1559.8	8.50	63.4	1592.8	13.2	13.8	1624.9	11.5
122.0	S_F	–	–	–	–	–	–	22.6	1559.2	8.74	63.4	1592.2	13.7	14.0	1625.0	11.6
145.0		81.5	1162.4	9.90	18.5	1190.7	9.50	22.2	1159.1	8.90	63.5	1592.3	14.0	14.3	1624.8	11.5
150.0	S_I	82.0	1162.5	10.0	18.0	1190.6	9.50	22.0	1559.3	9.00	63.5	1592.5	14.1	14.5	1625.0	11.9
154.0	S_C	83.7	1162.4	9.30	16.3	1190.5	10.8	19.5	1559.4	9.30	65.5	1592.7	14.8	15.0	1625.1	13.9
163.0		84.0	1162.2	8.86	16.0	1190.2	9.62	18.0	1559.7	9.30	66.6	1592.7	14.9	15.4	1625.4	10.3
190.0	S_A	84.5	1162.3	8.90	15.5	1190.4	9.60	16.2	1559.8	9.50	68.0	1592.7	15.0	15.8	1625.3	11.3
199.0	Iso	85.0	1162.0	9.00	15.0	1190.3	9.70	15.7	1559.5	10.4	68.5	1592.2	16.0	15.8	1624.9	11.5

PP – Peak Position; II – Integrated Intensity; LW – Linewidth (FWHM).

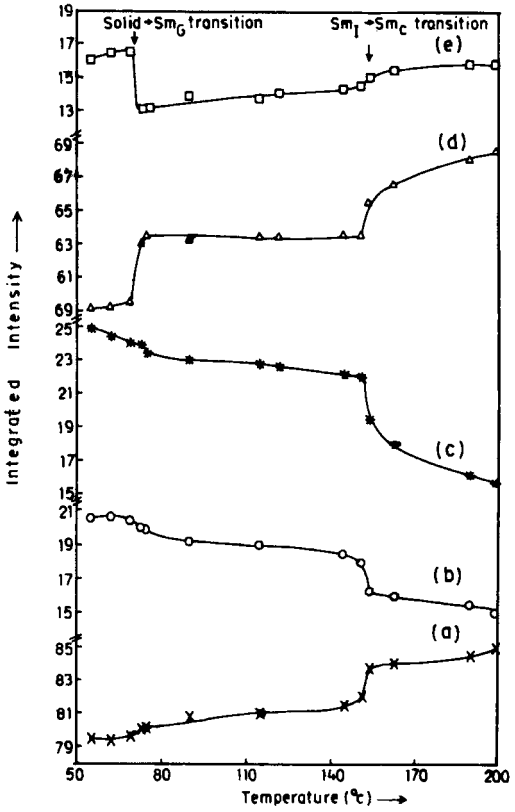

FIGURE 2 Variation of integrated intensity, taken as percent contribution of the individual band to its respective spectral region; (a) 1165 cm^{-1}, (b) 1195 cm^{-1}, (c) 1563 cm^{-1}, (d) 1594 cm^{-1}, (e) 1625 cm^{-1} bands.

(K–S_G transition here), the core part of the molecule is still expected to be rigid with very small orientational freedom. The smectic G phase has a pseudo-hexagonal packing, with a local herringbone structure [16–17]. The time scale involved is 10^{-11} s leading to an effectively hexagonal symmetry for S_G phase [16]. In this phase, even though translational freedom between molecules is almost nil [16], the lateral gap, that exists between each pseudo-hexagonally packed cluster [17] may facilitate the long alkyl chains to move more freely thereby producing alkyl tail strain on the core (specially peripheral benzene rings) affecting its characteristic Raman modes. The abnormality shown by some core connected Raman bands at the K–S_G transition may be due to this relatively free movement of the alkyl chains in S_G phase.

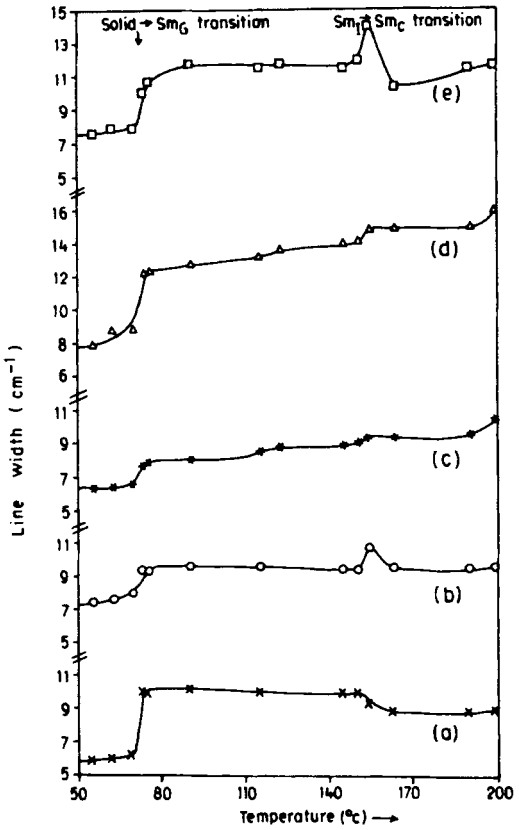

FIGURE 3 Variation of the linewidth (full width at half maximum) of Raman bands with temperature; (a) 1165 cm^{-1}, (b) 1195 cm^{-1}, (c) 1563 cm^{-1}, (d) 1594 cm^{-1}, (e) 1625 cm^{-1} bands.

A careful examination of Figure 4 reveals that at the $K-S_G$ transition the peak position of the 1195 cm^{-1} band ($\nu_{\phi-N}$) shifts by $\approx 5\,cm^{-1}$ towards lower frequency indicating a decrease in the energy of the ϕ — N= bond (loosening of bond). Increased orientational freedom of the long alkyl chain due to decrease in intermolecular interactions may put strain on the whole core part and thus soften the ϕ — N= bond. However, the integrated intensity of this mode does not show any abrupt change (see Fig. 2) indicating no appreciable charge distortion around the ϕ —N= bond at this phase transition. The 1625 cm^{-1} band ($\nu_{C=N}$) shows an abrupt decrease in integrated intensity near the $K-S_G$ transition (Fig. 2) which indicates that the π-electron cloud over —C=N— bond might have been distorted slightly due to strain exerted by the long alkyl chain on melting.

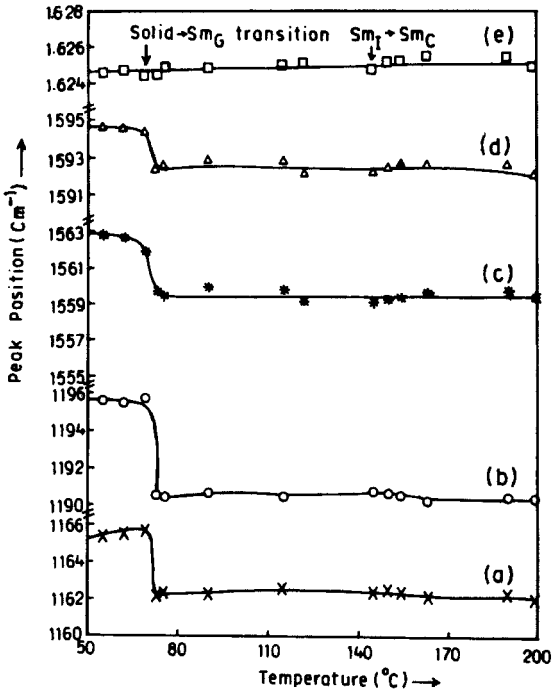

FIGURE 4 Variation of the peak position of Raman bands with temperature; (a) 1165 cm^{-1}, (b) 1195 cm^{-1}, (c) 1563 cm^{-1}, (d) 1594 cm^{-1}, (e) 1625 cm^{-1} bands.

However, the peak position of the $\nu_{C=N}$ does not show any appreciable shift (see Fig. 3) owing to the fact that the total energy of the bond remains unchanged. The three benzene modes ν_{9a} (1165 cm^{-1}), $\nu_{8a'}$(1563 cm^{-1}) and ν_{8a}(1594 cm^{-1}) also show some abnormality near $K-S_G$ transition in terms of frequency shifts towards lower side indicating softening of these modes. However, the ν_{8a} mode shows a jump in integrated intensity (see Fig. 2) indicating a possibility of charge drift from —C=N— towards benzene ring side. When we look at the linewidth data, it is seen from Figure 3 that linewidths of all the above mentioned bands show sudden jump at the $K-S_G$ transition. This may be due to the effect of increased orientational/vibrational freedom of long alkyl chains at the transition, especially on the peripheral benzene rings as well as on the ϕ — N — and — C= N — bonds. Due to this effect, the individual frequencies of the $\nu_{\phi-N}$, $\nu_{C=N}$ and the benzene ring modes differ from their original values, which in turn, broaden the linewidths of respective modes at the $K-S_G$ transition. Hence, it can be concluded that all these changes observed in the core connected

Raman modes at the $K-S_G$ transition are due to the effect of increased orientational/vibrational freedom of the long alkyl chain upon the core part of the molecule.

B. Smectic *I*–Smectic *C* Transition and the Evidence of Core Disorder

S_I-S_C transition is first order in nature [14–15] and is an example of transformation of an ordered tilted structure with hexagonal packing of molecules within the layers to a disordered tilted structure in smectic-smectic transitions. The two dimensional liquid like structure of S_C phase possesses a short range correlation between the molecular positions within the layer over a certain distance (known as a cluster). Because of the fluid character, neither the distance between the centers of the clusters is related to the local spacing nor are the intermolecular interactions correlated [17]. The intermolecular interactions being weak in this phase (S_C), the appreciable effects observed in the Raman modes during this transition are expected to arise from intramolecular dynamics. Taking these aspects into consideration, the possibility of intramolecular rotation around the molecular long axis along a flexible single bond inside the core can not be ruled out. This is, in fact, evident from the variation of linewidths and integrated intensities of some modes with temperature, during this transition.

Figure 3 reveals that linewidths of all the five Raman bands at 1165, 1195, 1563, 1594 and 1625 cm^{-1} exhibit small but noticeable change at the S_I-S_C transition. However, these changes are prominent and distinct for the $\nu_{\phi-N}$ and $\nu_{C=N}$ modes than those for the benzene ring modes. As it is known that Raman linewidth is a cumulative effect of linewidths originating from the temperature-independant vibrational dephasing and temperature-dependant reorintational motion, there must be some rotational/orientational motion occurring around the $\phi-N=$ or $-C=N-$ bonds in the liquid like phases which may be responsible for changes in the linewidths of these modes at the S_I-S_C transition. As the $\phi-N=$ bond is a single bond, the reorientational motions are much easier around this bond. Taking this aspect into consideration in our earlier study [19], we have calculated the activation energy for the reorientational motion around the $\phi-N=$ bond from the estimated contribution of the orientational motion to the Raman linewidth using standard methods [20–21]. We found that the temperature corresponding to this activation energy is reasonably close to the S_I-S_C transition temperature in TBDA [19] which indicates that the S_I-S_C transition is linked with a rotation around the $\phi-N=$ bond.

Figure 2 shows that the integrated intensity of the $\nu_{\phi-N}$ mode suddenly decreases at the $S_I - S_C$ transition temperature (154°C). This indicates appreciable distortion of σ-electron cloud over the ϕ—N= bond due to rotation about this bond. The integrated intensity of the $\nu_{C=N}$ mode increases slightly (see Fig. 2) indicating that the π-electron cloud regained its original value by accepting some electron density from the ϕ — N = bond. The integrated intensity of the $\nu_{8a'}$ mode decreases at this transition which shows that the rotation along the ϕ — N = bond helps the peripheral benzene rings to reorient along the flexible single bond causing slight distortion in their π-electron cloud. However, the integrated intensity of the ν_{8a} mode shows a jump in its value owing to the fact that ν_{8a} and $\nu_{8a'}$ modes are a pair of doubly degenerate mode and that decreases in integrated intensity in one is associated with an increase in the other.

The rotation around the ϕ — N = bond can lead to a modified structure of the core of the TBDA molecules in all its liquid like phases (S_C, S_A, isotropic *etc.*). Intermolecular interactions being comparatively weak and lesser steric hindrance in liquid phase, the long alkyl chains may try to stabilize themselves in the lowest energy configuration by reorienting the peripheral benzene rings around a flexible single bond (ϕ — N =) without affecting its backbone geometry significantly. This process which affects the Raman modes associated with the core indicates core disorder meaning thereby that the core no longer retains its original rigid character. However, this modified dynamics of the core still does not involve any serious modification of the molecule as a whole at the transition because the peak positions of all the core connected Raman bonds hardly show any anomaly (Fig. 3) during this transition ($S_I - S_C$), indicating that the total energy of respective bonds involved in the vibration remains unchanged. Moreover, this core disorder behaviour is also reflected in the form of a small but noticeable jump in the S_{ZZ} parameter (core order parameter) near the $S_C - S_A$ phase transition which is weakly first order in nature [22–24], in NMR study using anthracene-d_{10} as a spin probe [25].

On increasing temperature above 154°C, the integrated intensity of the $\nu_{8a'}$ mode (see Fig. 2) decreases steadily up to the isotropic phase due to the induced rotation about the ϕ — N = bond with increased fluidity, whereas the integrated intensity of the ν_{8a} mode increases gradually from solid to isotropic phase. The reason is quite obvious as discussed above. The integrated intensity of the $\nu_{C=N}$ mode increases slowly and attains a value in the isotropic phase which is close to its value in the solid phase. However, the linewidths of the $\nu_{\phi-N}$ and $\nu_{C=N}$ modes which show some peak like characteristics near the $S_C - S_I$ transition (> 54°C) on their increasing trend

of profiles are ascribed to the fact that the $S_I - S_C$ transition is not a purely first order type, rather it involves some second order characteristics [19].

Acknowledgements

Financial support from Department of Science and Technology, New Delhi is acknowledged.

References

[1] M. Fontana and S. Bini, *Phys. Rev. A*, **14**, 1555 (1976).
[2] W. J. Borer, S. S. Mitra and C. W. Brown, *Phys. Rev. Lett.*, **27**, 379 (1971).
[3] B. J. Bulkin and F. T. Prochaska, *J. Chem. Phys.*, **54**, 635 (1971).
[4] N. M. Amer, Y. R. Shen and H. Rosen, *Phys. Rev. Lett.*, **24**, 718 (1970).
[5] N. M. Amer and Y. R. Shen, *Solid State Comm.*, **12**, 263 (1973).
[6] D. Dvorjetski, V. Volterra and E. Wiener-Avnear, *Phy. Rev. A*, **12**, 681 (1975).
[7] B. J. Bulkin, D. Grunbaum, T. Kennelly and W. B. Loc, *Int. Liq. Cryst. Conf. Pramana Supp.*, **1**, Ed. S. Chandrasekhar (1975) p. 155.
[8] J. M. Schnur, *Phys. Rev. Lett.*, **29**, 1141 (1972).
[9] J. M. Schnur, *Mol. Cryst. Liq. Cryst.*, **23**, 155 (1973).
[10] N. M. Amer and Y. R. Shen, *J. Chem. Phys.*, **56**, 2654 (1972).
[11] Akihiko Sakamoto, Katsumi Yosino, Uichi Kubo and Yoshio Inuishi, *Japan J. Appl. Phys.*, **13**, 1691 (1974).
[12] J. M. Schnur, J. P. Sheridan and M. Fontana, *Proc. Int. Liq. Cryst. Conf. Pramana Supp.*, **1**, Ed. S. Chandrasekhar (1975) p. 175.
[13] J. M. Schnur and M. Fontana, *J. Phys.* (France), **35**, L-35 (1974).
[14] L. Leibert, *Liq. Cryst. Solid State Phys. Suppl.*, 14, Academic Press (1978).
[15] P. R. Alapati, D. M. Potukuchi, N. V. S. Rao, V. G. K. M. Pisipati and D. Saran, *Mol. Cryst. Liq. Cryst.*, **146**, 111 (1987).
[16] G. Vertogen and W. H. de Jeu, Thermotropic Liquid Crystal, Fundamentals Springer series in *Chemical Physics*, **45** (1975).
[17] G. W. Gray and J. W. Goodby, Smectic Liquid Crystals (Leonard Hill, London, 1984).
[18] G. Vertogen, *Adv. Raman Spectrosc.*, **1**, 219 (1972).
[19] S. K. Dash, Ranjan K. Singh, P. R. Alapati and A. L. Verma, *J. Physics: Condensed Matter*, **2**, 7802 (1997).
[20] A. V. Rakov, *Proc. Lebedev Phys. Int.*, **27**, 111 (1965).
[21] S. Sathiah, V. N. Sarin and H. D. Bist, *J. Physics: Condensed Matter*, **10**, 7829 (1989).
[22] J. Doucet, A. M. Levelut and M. Lambert, *Phy. Rev. Lett.*, **32**, 301 (1974).
[23] S. Krishna Prasad, V. N. Raja, V. S. Shankar Rao, Geeta G. Nair and M. E. Neubert, *Phys. Rev. A*, **42**, 2479 (1990).
[24] A. Wiegeleben, L. Richer, J. Deresch and D. Demus, *Mol. Cryst. Liq. Cryst.*, **59**, 329 (1980).
[25] P. R. Alapati and G. R. Luckhurst (unpublished results).